journal

J. Am. Ceram. Soc., **94** [9] 2933–2938 (2011)
DOI: 10.1111/j.1551-2916.2011.04450.x

Microwave Dielectric Properties of $Ba_2Ca_{1-x}Sr_xWO_6$ Double Perovskites

Yuanyuan Zhou,[‡] Siqin Meng,[‡] Hongchao Wu,[§] and Zhenxing Yue[†,‡]

[‡]State Key Laboratory of New Ceramics and Fine Processing, Department of Materials Science and Engineering, Tsinghua University, Beijing 100084, China

[§]School of Materials Science and Engineering, University of Science and Technology Beijing, Beijing 100084, China

$Ba_2Ca_{1-x}Sr_xWO_6$ ($x = 0$–1) microwave dielectric ceramics have been prepared using the two-step solid-state reaction method. The substitution of Sr^{2+} for Sr^{2+} can effectively lower the densification temperature of the ceramics from 1500° to 1200°C. Single-phase ceramics with double perovskite structures were obtained, and structural transitions occurred in $Ba_2Ca_{1-x}Sr_xWO_6$ via the phase sequence: cubic→rhombohedral→monoclinic with an increase of x. The microwave dielectric properties of the $Ba_2Ca_{1-x}Sr_xWO_6$ ceramics can be effectively tuned by tailoring x. The dielectric constant (ε_r) remains almost unvaried, the quality factor ($Q \times f$) decreases monotonically, and the temperature coefficient of resonant frequency (τ_f) changes in sign with the increase of x. A good combination of the microwave dielectric properties was obtained for $Ba_2Ca_{0.975}Sr_{0.025}WO_6$ sintered at 1250°C: $\varepsilon_r = 23.9$, $Q \times f = 80\ 200$ GHz, and $\tau_f = +18$ ppm/°C.

I. Introduction

MANY works have been focusing on developing dielectric materials with high dielectric constant (ε_r), high quality factor ($Q \times f$), and near zero temperature coefficient of resonant frequency (τ_f) to be used for dielectric resonators, oscillators, and filters at microwave frequencies.[1–2] $A_3B'B''_2O_9$ complex perovskites (where A = Ba, Sr; B′ = Mg, Zn, Ni, Co; B″ = Nb, Ta) are one of the most investigated materials because of the outstanding and tunable dielectric properties present in a number of compositions.[3–14] The highest reported Q values have been observed in these systems that exhibit the so-called 1:2 type of cation order on the B-sites. It is revealed that the good dielectric properties of these materials are related closely to the B-site cation ordering. However, to obtain a high degree of ordering, prolonging high-temperature sintering and soaking time or introducing small amounts of dopants is often necessary, which is not suitable for practical applications. Moreover, microwave dielectric properties of some 1:1 ordered perovskites with a general formula $A_2(B'B'')O_6$ (A = Ba, Sr, Ca; B′ = lanthanides and Y, B″ = Nb, Ta) were also investigated.[15–17] It is concluded that ionic ordering driving force is favored by larger differences in charges and ionic radii between the two B-site ions. Recently, the dielectric properties of tungstate-based double perovskites with the general formula $A_2(B'W)O_6$ (A = Ba, Sr, Ca; B′ = Mg, Co, Zn, Ni) have been reported.[18–20] Most of the compounds are characterized by a cubic perovskite structure, with an almost complete 1:1 ordering between the B-site ions. The B-site ordering is much easier to achieve for those double perovskites.

Considerable effort has been made toward understanding the relationship between microwave dielectric properties and the structure of the complex perovskite materials to gain better insight into the basic factors that influence the dielectric properties.[19–23] In general, tolerance factor (t) is used as a measure of the stability of the perovskite phases, which influences the structure and then the dielectric properties.

Double perovskite $Ba_2Ca_{1-x}Sr_xWO_6$ undergoes a phase transition with an increase of x.[24] To the best of our knowledge, no investigations on the microwave dielectric properties of Ba_2CaWO_6 or Ba_2SrWO_6 have been carried out. This spurs us to examine how the structure symmetry in the double perovskites influences the microwave dielectric properties. Then, the relationship between dielectric properties and t can be established, which will be helpful for the development of structure–property correlations. In addition, the systematic study of $Ba_2Ca_{1-x}Sr_xWO_6$ may reveal potentially useful materials for microwave applications. In the present work, the sintering behavior, microstructure, and microwave dielectric properties of the $Ba_2Ca_{1-x}Sr_xWO_6$ ceramics were investigated. The influence of crystal structure on the microwave dielectric properties of $Ba_2Ca_{1-x}Sr_xWO_6$ was discussed.

II. Experimental Procedure

Samples of $Ba_2Ca_{1-x}Sr_xWO_6$ ($x = 0$–1) were prepared using a precursor route. High-purity $BaCO_3$ (>99%), $CaCO_3$ (>99%), $SrCO_3$ (>99%), and WO_3 (>99.99%) chemicals were used as raw materials. First, $CaWO_4$ and $SrWO_4$ were prepared as precursors by calcining mixtures of $CaCO_3$, $SrCO_3$, and WO_3 chemicals at 800°C for 4 h, respectively. Secondly, nominal amounts of $BaCO_3$, $CaWO_4$, and $SrWO_4$ were weighed, ground, and calcined at 1000°C for 4 h. The calcined powder was remilled and dried. The resultant powder was added with a polyvinyl alcohol (5 wt%) solution as a binder and palletized into cylindrical pellets of 10 mm diameter and 6 mm thickness under a uniaxial pressure of 200 MPa. These pellets were debindered at 600°C for 4 h, and then sintered in the temperature range of 1150°–1500°C in air for 4 h.

The bulk densities of the sintered ceramics were measured using the Archimedes method. The crystal structures were determined by X-ray diffraction (XRD), using Cu$K\alpha$ radiation (D/Max-2500, Rigaku, Tokyo, Japan). Selected area electron diffraction (SAED) patterns were recorded in a transmission electron microscope (Tecnai G2 20, FEI, Hillsboro, OR), operating at 200 kV. The microstructure was observed by scanning electron microscopy (JSM-6301F, JEOL, Tokyo, Japan), and the chemical component elements were characterized by an energy-dispersive spectrometer (EDS) attached to the SEM. Raman spectra were excited with an argon laser and recorded using a Raman spectrometer (HR800, Horiba Jobin Yvon, Villeneuve D'ascq, France). Microwave dielectric properties of the polished

X. M. Chen—contributing editor

Manuscript No. 27967. Received May 4, 2010; approved January 20, 2011.
This work was financially supported by the Natural Science Foundation of China (Grant Nos. 50972074, 50921061, and 50672043), the Ministry of Science and Technology of China (through 973-Project under 2009CB623306), and China Postdoctoral Science Foundation (Grant No. 20090450352).
[†]Author to whom correspondence should be addressed. e-mail:yuezhx@mail.tsinghua.edu.cn

samples were determined using a network analyzer (HP8720ES, Hewlett-Packard, Santa Rosa, CA). The dielectric constants were measured using the Hakki–Coleman postresonator method by exciting the TE_{011} resonant mode of the dielectric resonators using the electric probe of an antenna as suggested by Courtney.[25,26] The unloaded quality factors were measured using the $TE_{01\delta}$ mode in the cavity method.[27] The temperature coefficients of τ_f were measured by noting the variation of resonant frequency of the TE_{011} mode in the reflection configuration over a temperature range of 25°–80°C.

III. Results and Discussion

$Ba_2Ca_{1-x}Sr_xWO_6$ ceramics were well sintered at 1500°C for $x = 0$, 1250°C for $x = 0.025$, 1225°C for $x = 0.05$, and 1200°C for $x = 0.1$–1, respectively. Figure 1 shows the XRD patterns of the well-sintered $Ba_2Ca_{1-x}Sr_xWO_6$ ceramics. It can be seen easily that every sample adopts a single perovskite structure, without any second phase detected within the detectable level of XRD. All superlattice lines indexed as (111), (311), (331), (511), and (531), respectively, exist in a double cubic cell, indicating the ordered arrangement of (Sr, Ca)O_6 and WO_6 octahedra. Moreover, the diffraction peaks shift to lower angles with an increase of x owing to the different ionic radii of Ca^{2+} (1.00 Å) and Sr^{2+} (1.18 Å).[28] According to Fu *et al.*,[24] the structural transition occurs in $Ba_2Ca_{1-x}Sr_xWO_6$ via a phase sequence: cubic–rhombohedral–monoclinic with an increase of x, which was derived from the splitting of the basic (222) and (400) reflections. It is said that neither the (222) reflection nor the (400) reflection splits for the cubic structure. The (222) reflection splits into a doublet with an intensity ratio of about 3:1 and the (400) reflection shows no splitting for the rhombohedral structure. The (222) reflection splits into a triplet and the (400) reflection into a doublet for the monoclinic structure. The enlarged region containing the basic (222) and (400) reflections shown in Fig. 1(b) indicates the phase transition compositions at $x = 0.1$ and 0.9, respectively.

As the deviation of rhombohedral and monoclinic perovskite structures from the cubic structure is very slight, an equivalent cubic cell about the three perovskite structures can be used in the research of some physical problems. The equivalent lattice parameter (a) and unit cell volume (V_m) of well-sintered $Ba_2Ca_{1-x}Sr_xWO_6$ were calculated, as shown in Fig. 2. It is obvious that the lattice parameter increases with increasing x, and the unit cell volume also increases accordingly because of the larger ionic radius of Sr^{2+} than Ca^{2+}.

Figure 3 shows the SAED patterns of the well-sintered $Ba_2Ca_{1-x}Sr_xWO_6$ ceramics, with $x = 0.025$, 0.05, and 0.9, respectively. All the maxima can be indexed on the basis of a double pseudocubic perovskite, in accordance with the XRD results.

Figure 4 shows the normalized Raman spectra of the well-sintered $Ba_2Ca_{1-x}Sr_xWO_6$ ceramics. Narrow and intense bands are usually observed for well-ordered structures. The 1:1 ordered perovskites with the *Fm*-3*m* symmetry allow the appearance of four Raman-active modes ($\Gamma(Fm\text{-}3m) = A_{1g}+E_g+2F_{2g}$).[29] As can be seen in Fig. 4(a), three main modes were observed for all samples. These results were observed previously in similar 1:1 ordered perovskites.[30,31] The lowest band at $\sim 103\ cm^{-1}$ corresponds to one of the F_{2g} modes, the weaker band at $\sim 410\ cm^{-1}$ corresponds to the other F_{2g} mode, and the highest band at $\sim 830\ cm^{-1}$ can be ascribed to the A_{1g} mode for cubic Ba_2CaWO_6, respectively. The E_g mode is too weak to be detected here. Raman spectra are suitable to study dynamic changes in the structure.[29] The F_{2g} modes should split into a doublet ($F_{2g} \rightarrow A_{1g}+E_g$) if the cubic *Fm*-3*m* symmetry is reduced.[29] Nine Raman-active modes were expected for the tetragonal *I*4/*m* symmetry and 24 for the monoclinic $P2_1/n$ structure, based on a new group-theory analysis.[31] Thus, more than four Raman-active modes are expected for the rhombohedral and monoclinic structures with a lower symmetry

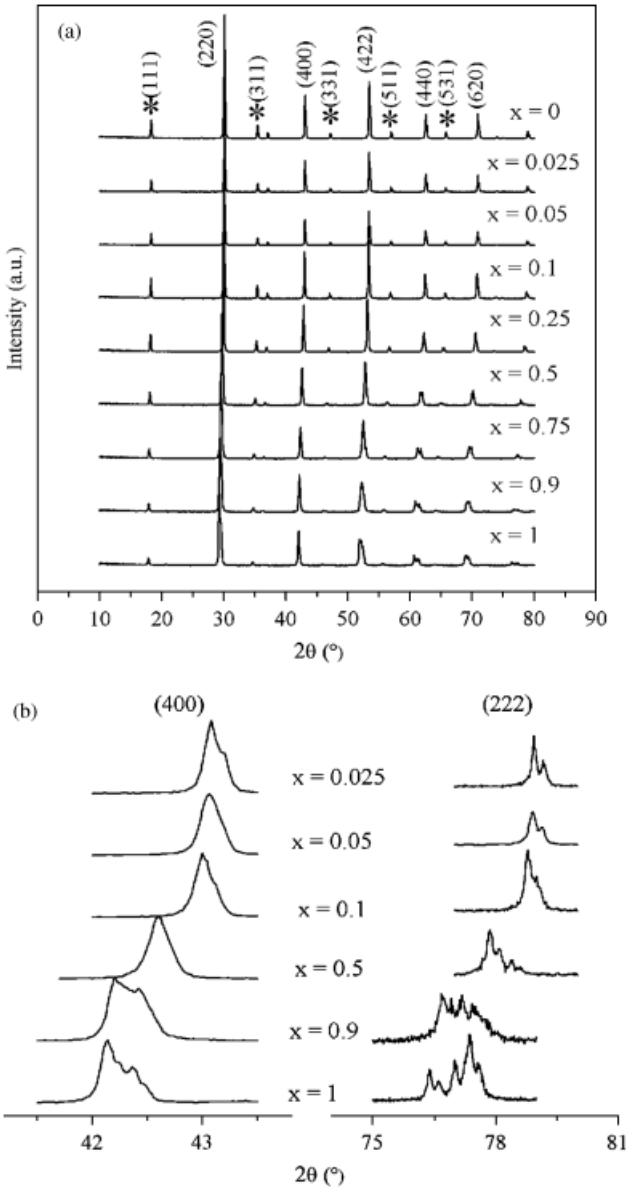

Fig. 1. XRD patterns (a) of well-sintered $Ba_2Ca_{1-x}Sr_xWO_6$ ceramics (*supper lattice reflections), and enlarged (222) and (400) reflection patterns (b) of some representative samples.

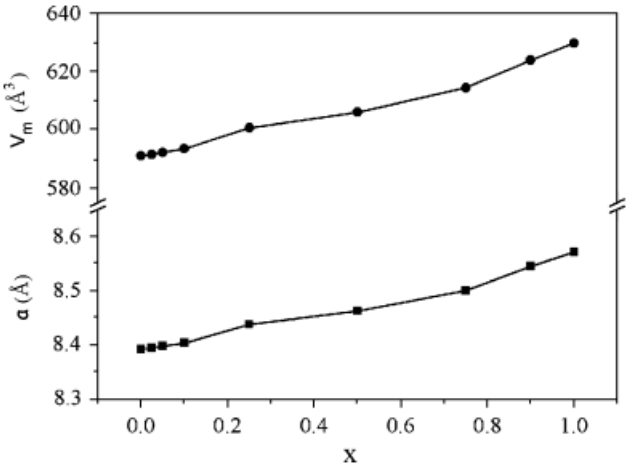

Fig. 2. Lattice parameter (a) and unit cell volume (V_m) of well-sintered $Ba_2Ca_{1-x}Sr_xWO_6$ ceramics vs. x.

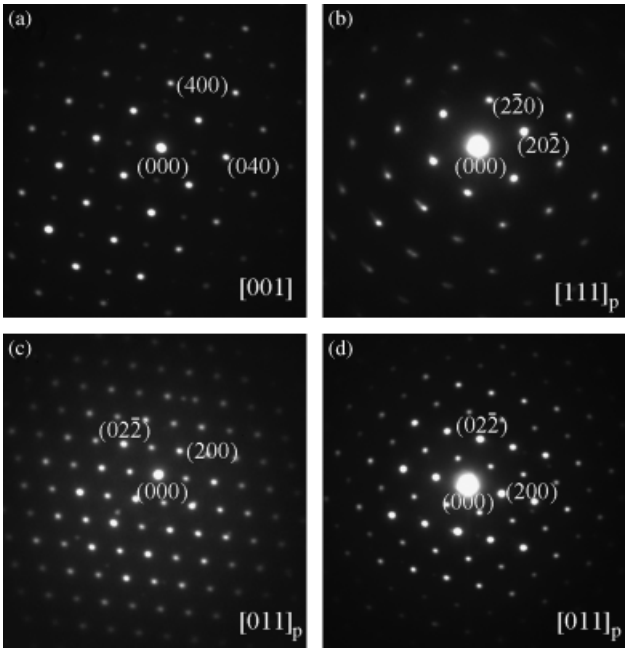

Fig. 3. SAED patterns of some well-sintered $Ba_2Ca_{1-x}Sr_xWO_6$ ceramics: (a) $x = 0.025$, (b) and (c) $x = 0.05$, and (d) $x = 0.9$. All maxima are indexed in a pseudocubic structure.

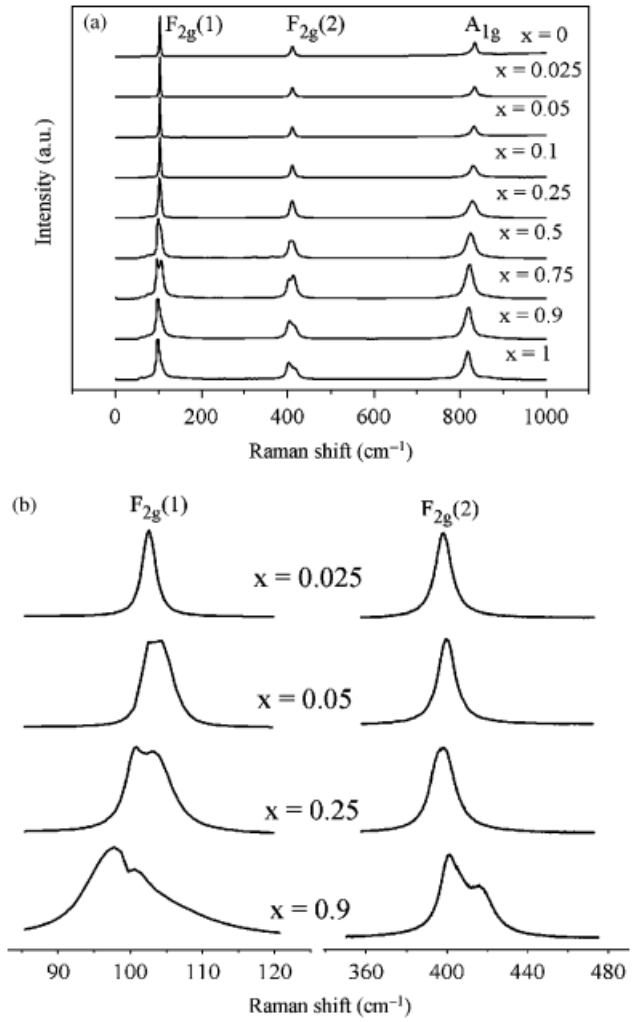

Fig. 4. Raman spectra (a) of well-sintered $Ba_2Ca_{1-x}Sr_xWO_6$ ceramics and enlarged F_{2g} mode patterns (b) of some representative samples.

than the cubic structure. In Fig. 4(b), an enlarged region containing both of the F_{2g} modes is shown. The splitting and broadening behavior of the F_{2g} modes further confirms the structure transitions in the $Ba_2Ca_{1-x}Sr_xWO_6$ matrix. For $x = 0.025$, no splitting of the modes was detected. The lower F_{2g} mode seems to split into a doublet for $x = 0.05$ and into a multiplet for $x = 0.9$. As the octahedral tilting is too small to be detected by XRD and appears to be sufficient to be detected by Raman spectroscopy,[31] the structure transition compositions of $Ba_2Ca_{1-x}Sr_xWO_6$ can be fixed at $x = 0.05$ and 0.9, respectively, based on the Raman results.

Figure 5 shows the SEM images and EDS spectra of some well-sintered $Ba_2Ca_{1-x}Sr_xWO_6$ ceramics. Small grains and several pores were observed for Ba_2CaWO_6 sintered at 1500°C (Fig. 5(a)). In contrast, pores are less for all the other samples, even with a small substitution ($x = 0.025$) of Sr^{2+} for Ca^{2+} (Fig. 5(b)). The grain size of the $Ba_2Ca_{1-x}Sr_xWO_6$ ($x > 0$) ceramics was influenced by both the sintering temperature and the Sr content. High sintering temperatures accelerate the grain growth (see Figs. 5(b)–(d)), while at the same sintering temperature, the grain size increases more markedly with the increase of x. Moreover, degradation in grain uniformity becomes more significant with a high Sr content (see Figs. 5(d)–(f)), which would damage its dielectric properties. The EDS spectrum for $x = 0.05$ shows Ba, Ca, Sr, and W signals, and that for $x = 1$ shows Ba, Sr, and W signals. This is consistent with the compositions.

Figure 6 and Table 1 show the relative density and microwave dielectric properties of the $Ba_2Ca_{1-x}Sr_xWO_6$ ceramics. It was confirmed that it was really hard to sinter Ba_2CaWO_6 into dense bodies. However, the substitution of Sr^{2+} for Ca^{2+} can efficiently reduce the sintering temperature of Ba_2CaWO_6, and all the $Ba_2Ca_{1-x}Sr_xWO_6$ ceramics with $x > 0$ were well sintered in the temperature range of 1200°–1250°C. As shown in Fig. 6, the relative densities of most $Ba_2Ca_{1-x}Sr_xWO_6$ ceramics are >97%. As Sr^{2+} is larger in size than Ca^{2+}, the instability of the crystal structure is induced by the Sr^{2+} substitution for Ca^{2+}, and lattice activation increases, which promotes the sintering of $Ba_2Ca_{1-x}Sr_xWO_6$. This may be the reason for the lower sintering temperature of $Ba_2Ca_{1-x}Sr_xWO_6$ ($x > 0$) ceramics. The dielectric properties of Ba_2CaWO_6 sintered at 1500°C were measured as $\varepsilon_r = 22.8$, $Q \times f = 22\ 800$ GHz, and $\tau_f = +46$ ppm/°C, and those of Ba_2SrWO_6 sintered at 1200°C were measured as $\varepsilon_r = 23.5$, $Q \times f = 39\ 700$ GHz, and $\tau_f = -34$ ppm/°C. By tailoring x, the dielectric properties of $Ba_2Ca_{1-x}Sr_xWO_6$ can be effectively tuned. The best combination of the microwave dielectric properties was obtained for $x = 0.025$: $\varepsilon_r = 23.9$, $Q \times f = 80\ 200$ GHz, and $\tau_f = +18$ ppm/°C.

The dielectric constants of the $Ba_2Ca_{1-x}Sr_xWO_6$ ceramics with $x > 0$ are between 23 and 24. In general, the dielectric constant is highly dependent on the relative density and ionic polarizability at microwave frequencies, and increases with an increase of B-site ionic polarizability.[13,20] It can be seen that the relative density of well-sintered $Ba_2Ca_{1-x}Sr_xWO_6$ ($x > 0$) is >97%; hence, its influence on the dielectric constant can be ignored. The relationship between dielectric constant and microscopic polarizability for cubic perovskites can be expressed through the Clausius–Mossotti formula,[32]

$$\frac{\varepsilon_r - 1}{\varepsilon_r + 2} = \frac{4\pi}{3}\frac{\alpha_m}{V_m} \tag{1}$$

where ε_r is the relative dielectric constant, α_m is the macroscopic polarizability, and V_m is the molar volume. The theoretical dielectric constant ε_{theo} calculated from Eq. (1) is also shown in Table 1. The deviation between ε and ε_{theo} is slight with a small value of x, and seems to increase with a large value of x due to a greater distortion from the cubic structure. Any deviation from cubic symmetry results in extra polarization; the larger the deviation from cubic symmetry, the larger the dielectric constant.[16] Thus, compared with the calculated dielectric constant ε_{theo}, the

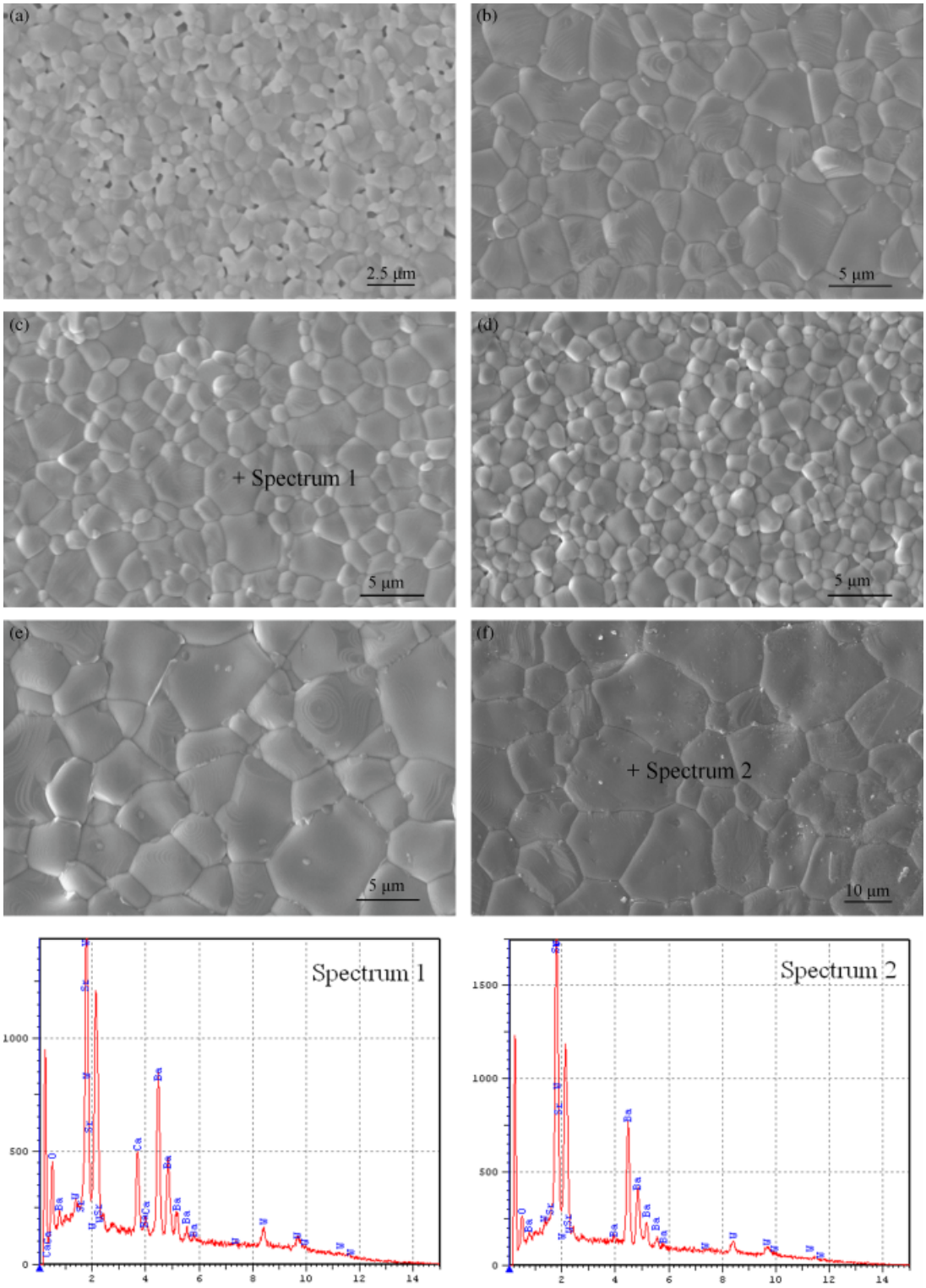

Fig. 5. SEM images of well-sintered $Ba_2Ca_{1-x}Sr_xWO_6$ ceramics: (a) $x = 0$, (b) $x = 0.025$, (c) $x = 0.05$, (d) $x = 0.1$, (e) $x = 0.5$, and (f) $x = 1$. EDS spectra where crosses mark are also shown.

real dielectric constant should be less changed with x. This is why the measured ε_r is almost unvaried.

However, the dielectric loss of $Ba_2Ca_{1-x}Sr_xWO_6$ is much more sensitive to x than the dielectric constant. Basically, the $Q \times f$ value of the well-sintered $Ba_2Ca_{1-x}Sr_xWO_6$ ceramics decreases monotonically with the increase of x. The dielectric loss measured represents the overall loss, including intrinsic loss related to the lattice anharmonicity and extrinsic contributions related to microstructure, second phase, porosity, etc.[33,34] Because the relative density is $>97\%$, and no second phase was detected, the effects of the density and second phase on $Q \times f$ for $Ba_2Ca_{1-x}Sr_xWO_6$ may be neglected. The decreased $Q \times f$ value may be related to the increase of lattice anharmonicity caused dielectric loss.[9,34,35] Moreover, the degradation in grain uniformity could result in dielectric loss, which also causes the $Q \times f$ value to decrease.

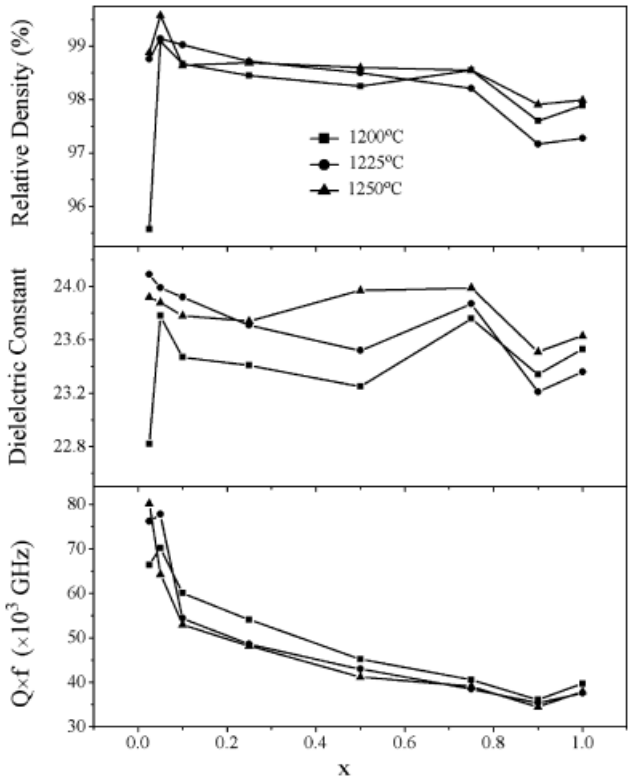

Fig. 6. Variations of relative density, dielectric constant, and $Q \times f$ value vs. x for $Ba_2Ca_{1-x}Sr_xWO_6$ ceramics.

The τ_f value of $Ba_2Ca_{1-x}Sr_xWO_6$ was not affected by the sintering temperature, but actually the composition. The composition induces a change in structure and then a change in the sign of τ_f, as shown in Table 1. In a perovskite structure, τ_f is closely related to oxygen octahedra tilting, which could be evaluated by the tolerance factor (t). For the $Ba_2Ca_{1-x}Sr_xWO_6$ system, t is defined as

$$t = \frac{R(\mathrm{Ba}) + R(\mathrm{O})}{\sqrt{2}\left[\frac{(1-x)R(\mathrm{Ca})+xR(\mathrm{Sr})+R(\mathrm{W})}{2} + R(\mathrm{O})\right]} \tag{2}$$

where R(Ba), R(Ca), R(Sr), R(W), and R(O) correspond to the ionic radii of Ba^{2+}, Ca^{2+}, Sr^{2+}, W^{6+}, and O^{2-}, respectively. The relationship between the temperature coefficient of dielectric constant (τ_ε) and the tolerance factor in Ba- and Sr-based complex perovskites was found by Reaney *et al.*,[22] whereas the data of $Ba_2Ca_{1-x}Sr_xWO_6$ were not included. To make a comparison, a graph of τ_ε vs. t for $Ba_2Ca_{1-x}Sr_xWO_6$ is shown in Fig. 7. Note that τ_ε was calculated by the equation

$$\tau_\varepsilon = -2(\tau_f + \alpha L) \tag{3}$$

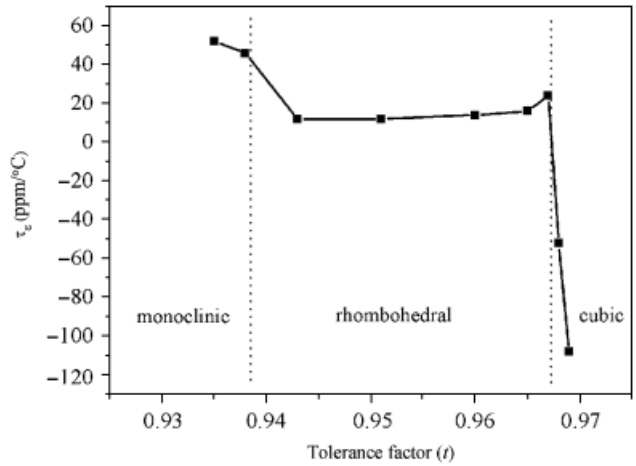

Fig. 7. Relationship of the τ_ε value vs. t for $Ba_2Ca_{1-x}Sr_xWO_6$ ceramics.

where α_L is the coefficient of linear thermal expansion. The α_L values are usually almost independent of composition for most ceramics; hence, a common value of 8 ppm/°C was used here. t was calculated using the Shannon ionic radii.[28] As a function of decreasing t, the phase transition sequence is considered to be cubic→rhombohedral→monoclinic. In the cubic phase region, τ_ε increases steeply as t decreases and changes in sign near the edge of the cubic stability range. After the onset of the cubic-rhombohedral phase transition, τ_ε varies slightly and is once again slightly close to zero. That is to say, the decrease of t does not result in a huge change in the value of τ_ε in the rhombohedral region. τ_ε increases abruptly again as t decreases with the onset of the rhombohedral–monoclinic phase transition, and then increases slightly in the monoclinic region. The trend of τ_ε variation vs. t is similar in nature to that observed in Ba- and Sr-based complex perovskites.[22] Therefore, it can be concluded that the onset of phase transitions is the major factor that influences the behavior of τ_ε as well as τ_f for $Ba_2Ca_{1-x}Sr_xWO_6$.

IV. Conclusions

$Ba_2Ca_{1-x}Sr_xWO_6$ ($x = 0$–1) double perovskites were prepared using a precursor route and their dielectric properties were studied in the microwave frequency range. Ba_2CaWO_6 has poor sinterability, and its sintering temperature is >1500°C, which leads to a low dielectric constant and $Q \times f$ value. The substitution of Sr^{2+} for Ca^{2+} can lower the sintering temperature and improve the sinterability; therefore, all the $Ba_2Ca_{1-x}Sr_xWO_6$ ($x > 0$) ceramics can be sintered into dense bodies in the temperature range of 1200°–1250°C. Furthermore, a structural transition in the $Ba_2Ca_{1-x}Sr_xWO_6$ system via the phase sequence: cubic→rhombohedral→monoclinic with an increase of x was confirmed by the XRD and Raman results.

Table I. Sintering Temperature, Relative Density, and Microwave Dielectric Properties of $Ba_2Ca_{1-x}Sr_xWO_6$ Ceramics

Composition x	Sintering temperature (°C)	Relative density (%)	f_0 (GHz)	ε_r	ε_{theo}	$Q \times f$ (GHz)	τ_f (ppm/°C)
0	1500	95.1	9.773	22.8	24.01	22 800	+46
0.025	1250	98.9	9.669	23.9	24.05	80 200	+18
0.05	1225	99.1	9.536	24.0	23.95	77 800	−20
0.1	1200	98.7	9.751	23.5	23.89	60 100	−16
0.25	1200	98.5	9.851	23.4	22.60	54 100	−15
0.5	1200	98.3	10.060	23.3	22.55	45 200	−14
0.75	1200	98.6	10.302	23.7	21.66	40 600	−14
0.9	1200	97.6	10.143	23.3	20.1	36 100	−31
1	1200	97.9	10.218	23.5	19.36	39 700	−34

The change in structure does not produce significant alterations in the dielectric constant, but does have a significance effect on $Q \times f$ and τ_f values. The $Q \times f$ value of the well-sintered $Ba_2Ca_{1-x}Sr_xWO_6$ ceramics decreases monotonically with the increase of x, which may be related to the increase of lattice-anharmonicity-caused dielectric loss. The τ_f value changes in sign with the increase of x. The onset of phase transitions is the major factor that influences the behavior of τ_f for $Ba_2Ca_{1-x}Sr_xWO_6$.

$Ba_2Ca_{0.975}Sr_{0.025}WO_6$ ceramics sintered at 1250°C for 4 h show excellent microwave dielectric properties: $\varepsilon_r = 23.9$, $Q \times f = 80\ 200$ GHz, and $\tau_f = +18$ ppm/°C. The low dielectric loss and the small τ_f value make the ceramics very promising in practical microwave applications.

References

[1]W. Wersing, "Microwave Ceramics for Resonators and Filters," *Curr. Opin. Solid State Mater. Sci.*, **1**, 715–31 (1996).

[2]R. J. Cava, "Dielectric Materials for Applications in Microwave Communications," *J. Mater. Chem.*, **11**, 54–65 (2001).

[3]S. Kawashima, M. Nishida, I. Ueda, and H. Ouchi, "$Ba(Zn_{1/3}Ta_{2/3})O_3$ Ceramics with Low Dielectric Loss at Microwave Frequencies," *J. Am. Ceram. Soc.*, **66**, 421–3 (1983).

[4]S. B. Desu and H. M. Obryan, "Microwave Loss Quality of $BaZn_{1/3}Ta_{2/3}O_3$ Ceramics," *J. Am. Ceram. Soc.*, **68**, 546–51 (1985).

[5]K. Endo, K. Fujimoto, and K. Murakawa, "Dielectric Properties of Ceramics in $Ba(Co_{1/3}\ Nb_{2/3})O_3$–$Ba(Zn_{1/3}Nb_{2/3})O_3$ Solid Solution," *J. Am. Ceram. Soc.*, **70**, C215–8 (1987).

[6]K. H. Yoon, D. P. Kim, and E. S. Kim, "Effect of $BaWO_4$ on the Microwave Dielectric Properties of $Ba(Mg_{1/3}Ta_{2/3})O_3$ Ceramics," *J. Am. Ceram. Soc.*, **77**, 1062–6 (1994).

[7]I. T. Kim, Y. H. Kim, and S. J. Chung, "Ordering and Microwave Dielectric Properties of $Ba(Ni_{1/3}Nb_{2/3})O_3$ Ceramics," *J. Mater. Res.*, **12**, 518–25 (1997).

[8]M. A. Akbas and P. K. Davies, "Ordering-Induced Microstructures and Microwave Dielectric Properties of the $Ba(Mg_{1/3}Nb_{2/3})O_3$–$BaZrO_3$ System," *J. Am. Ceram. Soc.*, **81**, 670–6 (1998).

[9]J. Venkatesh and V. R. K. Murthy, "Microwave Dielectric Properties of (Ba, Sr)$(Zn_{1/3}Ta_{2/3})O_3$ Dielectric Resonators," *Mater. Chem. Phys.*, **58**, 276–9 (1999).

[10]R. I. Scott, M. Thomas, and C. Hampson, "Development of Low Cost, High Performance $Ba(Zn_{1/3}Nb_{2/3})O_3$ Based Materials for Microwave Resonator Applications," *J. Eur. Ceram. Soc.*, **23**, 2467–71 (2003).

[11]M. Bieringer, S. M. Moussa, L. D. Noailles, A. Burrows, C. J. Kiely, M. J. Rosseinsky, and R. M. Ibberson, "Cation Ordering, Domain Growth, and Zinc Loss in the Microwave Dielectric Oxide $Ba_3ZnTa_2O_9$," *Chem. Mater.*, **15**, 586–97 (2003).

[12]C.-W. Ahn, H.-J. Jang, S. Nahm, H.-M. Park, and H.-J. Lee, "Effects of Microstructure on the Microwave Dielectric Properties of $Ba(Co_{1/3}Nb_{2/3})O_3$ and $(1-x)Ba(Co_{1/3}Nb_{2/3})O_3$–$x$ $Ba(Zn_{1/3}Nb_{2/3})O_3$ Ceramics," *J. Eur. Ceram. Soc.*, **23**, 2473–8 (2003).

[13]M. W. Lufaso, "Crystal Structures, Modeling, and Dielectric Property Relationships of 2:1 Ordered $Ba_3M'M_2O_9$ (M′ = Mg, Ni, Zn; M″ = Nb, Ta) Perovskites," *Chem. Mater.*, **16**, 2148–56 (2004).

[14]M. S. Fu, X. Q. Liu, and X. M. Chen, "Effects of Mg Substitution on Microstructures and Microwave Dielectric Properties of $Ba(Zn_{1/3}Nb_{2/3})O_3$ Perovskite Ceramics," *J. Am. Ceram. Soc.*, **93**, 787–95 (2010).

[15]M. Takata and K. Kageyama, "Microwave Characteristics of $A(B^{3+}_{1/2}B^{5+}_{1/2})O_3$ Ceramics (A = Ba, Ca, Sr; B^{3+} = La, Nd, Sm, Yb; B^{5+} = Nb, Ta)," *J. Am. Ceram. Soc.*, **72**, 1955–9 (1989).

[16]L. Abdul Khalam, H. Sreemoolanathan, R. Ratheesh, P. Mohanan, and M. T. Sebastian, "Preparation, Characterization and Microwave Dielectric Properties of $Ba(B'_{1/2}Nb_{1/2})O_3$ [B′ = La, Pr, Nd, Sm, Eu, Gd, Tb, Dy, Ho, Y, Yb and In] Ceramics," *Mater. Sci. Eng. B*, **107**, 264–70 (2004).

[17]L. Abdul Khalam and M. T. Sebastian, "Low Loss Dielectrics in the $Ca(B'_{1/2}Nb_{1/2})O_3$ [B′ = Lanthanides, Y] System," *J. Am. Ceram. Soc.*, **90**, 1467–74 (2007).

[18]J. J. Bian, K. Yan, and Y. F. Dong, "Microwave Dielectric Properties of $A_{1-3x/2}La_x(Mg_{1/2}W_{1/2})O_3$ (A = Ba, Sr, Ca; $0.0 \le x \le 0.05$) Double Perovskites," *Mater. Sci. Eng. B*, **147**, 27–34 (2008).

[19]D. D. Khalyavin, J. Han, A. M. R. Senos, and P. Q. Mantas, "Synthesis and Dielectric Properties of Tungsten-Based Complex Perovskites," *J. Mater. Res.*, **18**, 2600–7 (2003).

[20]F. Zhao, Z. X. Yue, Z. L. Gui, and L. T. Li, "Preparation, Characterization and Microwave Dielectric Properties of A_2BWO_6 (A = Sr, Ba; B = Co, Ni, Zn) Double Perovskite Ceramics," *Jpn. J. Appl. Phys.*, **44**, 8066–71 (2005).

[21]E. L. Colla, I. M. Reaney, and N. Setter, "Effect of Structural Changes in Complex Perovskites on the Temperature Coefficient of the Relative Permittivity," *J. Appl. Phys.*, **74**, 3414–25 (1993).

[22]I. M. Reaney, E. L. Colla, and N. Setter, "Dielectric and Structural Characteristics of Ba- and Sr-Based Complex Perovskites as a Function of Tolerance Factor," *Jpn. J. Appl. Phys.*, **33**, 3984–90 (1994).

[23]I. M. Reaney and R. Ubic, "Dielectric and Structural Characteristics of Perovskites and Related Materials as a Function of Tolerance Factor," *Ferroelectrics*, **228**, 23–38 (1999).

[24]W. T. Fu, S. Akerboom, and D. J. W. IJdo, "Crystal Structures of the Double Perovskites $Ba_2Sr_{1-x}Ca_xWO_6$," *J. Solid State Chem.*, **180**, 1547–52 (2007).

[25]B. W. Hakki and P. D. Coleman, "A Dielectric Resonator Method of Measuring Inductive Capacitance in the Millimeter Range," *IEEE Trans. Microwave Theory Technol.*, **8**, 402–10 (1960).

[26]W. E. Courtney, "Analysis and Evaluation of a Method of Measuring the Complex Permittivity and Permeability of Microwave Insulators," *IEEE Trans. Microwave Theory Technol.*, **18**, 476–85 (1970).

[27]J. Krupka, K. Derzakowski, B. Riddle, and J. B. Jarvis, "A Dielectric Resonator for Measurements of Complex Permittivity of Low Loss Dielectric Materials as Function of Temperature," *Meas. Sci. Technol.*, **9**, 1751–6 (1998).

[28]R. D. Shannon, "Revised Effective Ionic Radii and Systematic Study of Inter Atomic Distances in Halides and Chalcogenides," *Acta Crystallogr.*, **A32**, 751–7 (1976).

[29]I. G. Siny, R. Tao, R. S. Katiyar, R. Y. Guo, and A. S. Bhalla, "Raman Spectroscopy of Mg–Ta Order–Disorder in $BaMg_{1/3}Ta_{2/3}O_3$," *J. Phys. Chem. Solid*, **59**, 181–95 (1998).

[30]I. Gregora, J. Petzelt, J. Pokorný, V. Vorlícek, Z. Zikmund, R. Zurmühlen, and N. Setter, "Raman Spectroscopy of the Zone Center Improper Ferroelastic Transition in Ordered $Ba(Y_{1/2}Ta_{1/2})O_3$ Complex Perovskite Ceramic," *Solid State Commun.*, **94**, 899–903 (1995).

[31]A. Dias, G. Subodh, M. T. Sebastian, M. M. Lage, and R. L. Moreira, "Vibrational Studies and Microwave Dielectric Properties of A-Site-Substituted Tellurium-Based Double Perovskites," *Chem. Mater.*, **20**, 4347–55 (2008).

[32]A. J. Bosman and E. E. Havinga, "Temperature Dependence of Dielectric Constants of Cubic Ionic Compounds," *Phys. Rev.*, **129**, 1593–60 (1963).

[33]R. Zurmühlen, J. Petzelt, S. Kamba, V. alentin, V. Voitsekhovskii, E. Colla, and N. Setter, "Dielectric Spectroscopy of $Ba(B'_{1/2}B_{1/2})O_3$ Complex Perovskite Ceramics: Correlations Between Ionic Parameters and Microwave Dielectric Properties. I. Infrared Reflectivity Study (10^{10}–10^{14} Hz)," *J. Appl. Phys.*, **77**, 5341–50 (1995).

[34]W. S. Kim, E. S. Kim, and K. H. Yoon, "Effects of Sm^{3+} Substitution on Dielectric Properties of $Ca_{1-x}Sm_{2x/3}TiO_3$ Ceramics at Microwave Frequencies," *J. Am. Ceram. Soc.*, **82**, 2111–5 (1999).

[35]J. Petzelt, S. Pacesova, J. Fousek, S. Kamba, V. Zelezny, V. Koukal, J. Schwarzbach, B. P. Gorshunov, G. V. Kozolov, and A. A. Volkov, "Dielectric Spectra of Some Ceramics for Microwave Applications in the Range of 10^{10}–10^{14} Hz," *Ferroelectrics*, **93**, 77–85 (1989). □